CORONAL MAGNETIC FIELD CONTEXT OF SIMPLE CMEs INFERRED FROM GLOBAL POTENTIAL FIELD MODELS

J. G. LUHMANN[1], YAN LI[1], XUEPU ZHAO[2] and SEIJI YASHIRO[3]
[1]*Space Sciences Laboratory, University of California, Berkeley, CA 94720, U.S.A.*
[2]*Center for for Space Science and Astrophysics, Stanford University, Palo Alto, CA 94305, U.S.A.*
[3]*The Catholic University of America, Washington DC 20064, U.S.A.*

(Received 13 September 2002; accepted 16 December 2002)

Abstract. Most work on coronal mass ejection (CME) interpretation focuses on the involved active region rather than on the large-scale coronal context. In this paper a global potential-field source-surface model of the coronal magnetic field is used to evaluate the sensitivity of the coronal field configuration to the location, orientation, and strength of a bipolar active region relative to a background polar field distribution. The results suggest that the introduction of antiparallel components between the field of the active region and the background field can cause significant topological changes in the large-scale coronal magnetic field resembling observations during some simple CMEs. Antiparallel components can be introduced in the real corona by the diffusion and convection of photospheric fields, flux emergence, or erupted or shear-induced twist of active-region fields. Global MHD models with time-dependent boundary conditions could easily test the stability of such configurations and the nature of any related transients.

1. Introduction

Over a decade has passed since Harrison *et al.* (1990) and Sime (1989), among others, concluded that coronal mass ejections, or CMEs, must be a manifestation of large-scale coronal magnetic field restructuring. Yet, in spite of a wealth of new, more detailed observations from the SOHO spacecraft, and a great increase in the analytical and numerical tools being brought to bear on the CME problem, a clear picture of their cause(s) and coronal setting(s) eludes us (e.g., Webb *et al.*, 1997; Subramanian and Dere, 2001; Zhao and Webb, 2002). Currently proposed physical concepts of CME initiation and early evolution include the so-called tether-cutting and breakout models, among others (see the recent review by Forbes, 2000, and references therein). In the meantime, the observations indicate that the Sun is highly inventive when it comes to setting up conditions for coronal eruptions. During the course of the solar cycle, the corona restructures repeatedly, with most frequency and intensity approaching and around solar maximum. Some of this restructuring is permanent, while some is fleeting. Similarly, some restructuring is abrupt and violent, while some is slow and quiescent. Tether-cutting and breakout may simply be two physical routes taken in the corona's ongoing processes of adjustment to the dynamo below, depending on the topology of the magnetic field.

Solar Physics **213:** 367–386, 2003.
© 2003 *Kluwer Academic Publishers. Printed in the Netherlands.*

There is little debate concerning control of the corona's structure by the magnetic field conditions at its lower boundary. Reconfigurations can either be driven by flux emergence from below the photosphere, and photospheric motions rearranging the field pattern, or occur due to an unstable arrangement of the resulting distribution of matter and fields in a region. The arguments mainly concern the relationships between particular kinds of photospheric field distributions and/or changes and CMEs. For example, some observational evidence points to emergence of cancelling magnetic flux in active regions as a CME-triggering event (Feynman and Martin, 1995). Vector magnetographs (e.g., Falconer, 2001), as well as numerical simulations experimenting with CME initiation (e.g., Linker and Mikić, 1995) indicate the necessary presence of twisted or non-potential fields on global and/or active region scales in both promoting coronal eruptions and determining their character (i.e., their speed, flux rope topology, the presence of prominence material). Yet these are advanced considerations when we have yet to fully explore the ways in which the steady corona is configured for various photospheric field distributions, and the sensitivity of those configurations to different types of changes in those distributions.

One major limitation on such studies is that global coronal MHD modeling is still in its infancy relative to magnetospheric MHD modeling. Virtually all 3D simulations (e.g., Usmanov, 1995; Linker and Mikić, 1995; Mikić *et al.*, 1999; Wu, Andrews, and Plunkett, 2001) have modest spatial resolution, simplified treatments of the state or energy equation and the related heat or momentum sources, and require significant computational resources for even single trials of a steady case. While progress is being made, it is worth experimenting with a much simpler model in the spirit of Priest (2001) and of Priest and Schrijver (1999), who focused on analyzing potentially unstable magnetic field topologies in local potential models of 'toy' active regions consisting of several bipoles on a plane.

We have been using the well-known potential-field source-surface model (e.g., Altschuler *et al.*, 1977; Wang and Sheeley, 1992) to approximate the large-scale coronal magnetic field around the times of CMEs in the potential limit (Luhmann *et al.*, 1998; Li *et al.*, 2001). Our particular focus has been on changes in the open/closed coronal field topology, under the assumption that newly opened field lines expand outward beyond the source surface during the CME. While this approach cannot describe the actual transient involved in the reconfiguration, plasma aspects of the corona, or the involvement of nonpotential features such as coronal current sheets or twisted fields, it gives useful first-order pictures of the coronal context of CMEs. The results moreover suggest that the global potential field model can be applied to examine the relationships between coronal structures such as helmet streamers and the involved active region(s). For example, Wang and Sheeley (1999) used a potential-field source-surface model to suggest how filament eruptions could result when emerging active-region fluxes rearrange the overlying large-scale coronal fields.

Here we describe a potential-field source-surface model analog for the simplest observed cases of CMEs occurring when one large bipolar active region is present on the photosphere. This idealized case study is exemplified by the solar minimum period August–November 1996 when the SOHO mission was in full operation, with all coronagraph, EUV telescope and magnetograph images available from the SOHO Archive at the Solar Data Analysis Center (*http://umbra.gsfc.nasa.gov*). Intervals from this period have been studied in the context of Whole-Sun Month (Gibson *et al.*, 1999), in efforts to model the prominence that appeared along the active-region neutral line (Aulanier *et al.*, 1999), and in the analysis of coronal streamers in coronagraph images with a potential-field source-surface model (Wang *et al.*, 1997). As seen in the CDAW CME-Catalogue at the NRL SOHO-LASCO website (*http://lasco-www.nrl.navy.mil/*), created and maintained by Seiji Yashiro, this period also included over 20 coronal eruptions, with 2 classified as halo events (also see Lewis and Simnett, 2000, for a discussion of CMEs during this period). The more complex case of a few bipoles on the photosphere is also touched upon.

We suggest that the participation of the bipolar active region in the helmet streamer belt configuration represents a potential for coronal restructuring akin to breakout. In this case the breakout is enabled when the active region initially embedded in the helmet streamer belt suddenly forms its own separate helmet structure. The key element in this change in global field topology is the relative orientation of the active region bipole with respect to the helmet streamer belt fields. When that orientation produces antiparallel fields and their associated nulls, a major topological change occurs in the magnetic cellular structure of the corona. The strength of the bipolar active region fields relative to the solar polar fields, the active region latitude, and the distribution of the solar polar fields are contributing factors. We suggest that such topological changes, brought about by bipolar active region footpoint motion or field twisting (and thus effective bipole reorientation), may underlie the simple CMEs observed in the period of observations surrounding the last solar minimum.

2. Approach

Priest and Schrijver (1999) (also Longcope and Kankelborg, 2001) stressed the importance of the cellular structure of the coronal magnetic field, with its separatrices, nulls, and complex connectivities, in setting up potentially unstable topologies around active regions. They note that ‘the eruption of flux from the Sun may even sometimes be due to a change of topology caused by emerging flux breakout’, an idea they attribute to Bungey (1995). A specific study by Beveridge, Priest, and Brown (2002), of the potential magnetic topologies of two bipolar regions of different strengths interacting with one another, is especially relevant to the present analysis. These authors find several distinct states of the cellular structure

of the surrounding fields, depending on the bipoles' relative positions, orientations, and strengths. As the bipoles in their study are point sources on a nonmagnetic plane, the attributes of pole separation and depth, and the role of a background or larger-scale field, are not a part of their analysis.

Antiochos (1998) discussed two examples of magnetic topologies for bipolar and delta-spot active regions with interacting large and active-region scale fields, concluding that the complex multipolar topology of the delta-region field is most susceptible to reconnection and disruption. Applying these ideas on topological complexity to a global scale, Antiochos, DeVore, and Klimchuk (1999) carried out a 2.5-D numerical simulation wherein eruption of a central sheared coronal arcade occurs in a global triple-arcade system. In the initial field configuration, the overlying large-scale arcade contains a magnetic null above the erupting central arcade. The consequence of the eruption is the 'breakout' of the central sheared arcade field, while the two bracketing arcades (now divided by the erupted central arcade) remain, bridging the space between the erupted arcade and the solar polar regions. This result will be seen to have a clear counterpart in the present study.

In the real corona, coronagraph and eclipse observations and models suggest that both a circumsolar coronal arcade, the helmet streamer belt, and other topologically distinct coronal helmets can exist. The helmet streamer belt geometry explains the solar rotation-modulated ray structures seen in white-light coronagraph images obtained around solar minimum (Wang *et al.*, 1997). The separate helmets occur only when the global field is more complex than a dipole. In contrast to the helmet streamer belt, they are surrounded by monopolar open magnetic fields as illustrated in Figure 1(a) from Antiochos (1998). Many of these separate helmets inferred from photospheric field observations and the potential-field source-surface model do not reach the source surface. However, when they do, they create a topology with a toroidal arcade and an associated closed loop neutral line on the source surface, analogous to Figure 1(b) from Antiochos (1998). This is in contrast to the helmet streamer belt, which by definition reaches the source surface at ~ 2.5 solar radii where its cusp defines the base of the heliospheric current sheet. Whether the secondary ring-shaped neutral lines inferred for the separate helmets exist and produce secondary streamer structures is an open question.

Both the helmet streamer belt and external helmets may participate in CMEs. Each possesses characteristics suggesting prospective instabilities: the helmet streamer belt because its photospheric boundaries are subject to constant change from differential rotation and photospheric flux emergence and disappearance-while antiparallel fields and a current sheet exist at its cusp, and the separate helmet because it harbors a null point near its apex. Even the coronal restructuring associated with the formation or disappearance of a large new magnetic cell or separate helmet could be considered an instability that precipitates a coronal transient. Below we infer that the coronal magnetic topology is prone to major reconfigurations involving the splitting of the helmet streamer and the separation of secondary helmets from the helmet streamer belt.

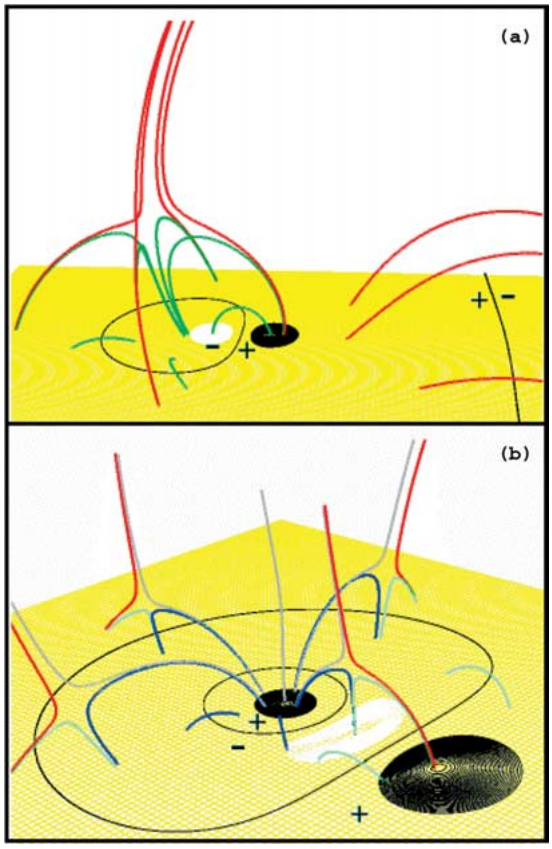

Figure 1. (a) Topology of a possible coronal field helmet structure separate from the helmet streamer belt, with a cusp and magnetic null point at its maximum altitude. (b) Another possible separate coronal helmet structure, but with a ring-shaped neutral line defining the apex of its last closed field arcade. Both of these configurations are surrounded by open fields of one polarity. These illustrations are reproduced from a paper by Antiochos (1998).

To examine the ways in which a global coronal field interacts with a single bipolar active region, we use a potential-field source-surface model with a standard spherical source surface at 2.5 $R_{\odot}$. This model has been described in earlier publications (e.g., Luhmann *et al.*, 1998; Li *et al.*, 2001) and so its details will not be repeated here. The present application of this model is in the use of constructed photospheric magnetic field maps rather than magnetograph-based synoptic maps. This technique was used many times by Sheeley, Wang, and Harvey (1989) and Wang and Sheeley (1993, 1999, 2002) to study topics ranging from the effects of active-region emergence on coronal holes (Sheeley, Wang, and Harvey, 1989), to the rigid rotation of coronal holes (Wang and Sheeley, 1993), to the origin and evolution of the open fields on the Sun (Wang and Sheeley, 2002; also see Mackay, Priest, and Lockwood, 2002).

In the present analysis we use monopole pairs of opposite signs to represent active regions in our constructed synoptic maps. These monopoles are scaled in strength in relation to the background field, and can be placed at various depths beneath the 'surface' of the map. The use of the monopoles both preserves the divergenceless magnetic field in the model and avoids sharp edges in the photospheric field distribution that add noise to the finite-spherical harmonic order field reconstructions. Their fields also resemble the observed fields of large bipolar active regions when the model poles are located a distance below the photosphere. We use background global fields that fall off with strength from the poles with a gaussian envelope. This allows us to mimic the sharper-than-dipolar concentration (e.g., Sheeley, Wang, and Harvey, 1989) of the observed photospheric polar fields, and is an important element of the model behavior.

Our constructed maps are input to the same routine that is used to calculate spherical harmonic coefficients from observation-based synoptic maps. It is found that 30 orders of harmonic coefficients are adequate for resolution of the large bipolar active regions produced by placing the monopoles at a depth 0.2 $R_\odot$ beneath the photosphere, with a separation of 14 deg. The model active-region peak field is $\sim 6-8$ times the peak polar field strength. A 25-deg width Gaussian falloff of the polar field, combined with the modeled bipolar region, produces maps that resemble observations.

Below we first explore how the combination of this single bipolar active region and the background photospheric field produce a variety of coronal magnetic field topologies depending on the active region latitude, inclination and strength. Interestingly, Mackay, Priest, and Lockwood (2002) have just published a highly complimentary analysis of the relationship of open coronal fields to the initial state and subsequent long-term evolution of a single bipolar active region. We find the most drastic changes in topologies include the separation of a topologically distinct helmet structure from the helmet streamer belt in a reconfiguration akin to the Antiochos, DeVore, and Klimchuk (1999) breakout model of CMEs. We then show that the modeled potential coronal field structures resulting from this topological change resemble some of the simple CMEs observed during August–November, 1996. These results can be used to both analyze consequences of the topological change (e.g., helmet streamer deflections and open field changes), and as a template for the study of more complex photospheric and coronal field CME scenarios.

3. Single Bipolar Active Region Scenario

The simple case of a single bipolar active region in a background magnetic field with polar concentrations can produce a variety of coronal features depending on the description of both the bipole and the background. As noted above, in constructing the counterpart of photospheric synoptic maps for our model experiments, we assumed that the bipole consists of a pair of monopoles separated by 14 deg,

both located at a depth of 0.2 solar radii beneath the plane of the photospheric synoptic map. The central longitude of the bipole is at 170 deg. The bipole latitude is a parameter of our experiment. The bipole axis tilt measured from east (toward smaller longitudes for the Sun) is also a parameter; the four tilt angles 0, 90, 180, and -90 deg sample the full range of possible field configurations from the bipole interaction with the background coronal magnetic field. The peak background polar field with its 25-deg width Gaussian latitudinal dependence is scaled to one for this study, and the active region bipole field strength scaled to that to obtain observationally consistent ratios for the two sources of flux (e.g., de Toma, White, and Harvey, 2000). The background field gradient is sufficiently steep that the active region fields dominate the constructed photospheric synoptic maps below ~ 65 deg latitude.

In view of the importance of active region bipole tilt in this study, it is important to note that twist may play the role of tilt in real active regions or in a corresponding nonpotential model. Also, an effective change of bipole axis tilt in a real synoptic map can be caused by differential rotation, diffusion and meridional convection acting on a decaying bipolar region, or from the emergence of new flux. Thus our use of bipole axis tilt as a parameter can be viewed as both showing coronal features for different steady cases and possible evolutionary trends. In the case of active region field twist related bipole reorientation, the relevant changes may not be fully detectable in scalar magnetograms.

Figures 2 and 3 show, in Carrington synoptic form, the coronal hole photospheric footprints, helmet streamer belt, and source-surface neutral line for the cases where the bipolar active region is placed at the equator, and at 30 deg north latitude, with bipole axis tilts of -90, 0, $+90$, and 180 deg. The gray shading in the left hand panels represents the presumed photospheric field distributions. Strong fields arising from the active region centers are indicated by the red field lines in the right-hand panels. Note that the modeled coronal hole footprints, shown in blue, are expected to be larger than on the real Sun because the background photospheric field is unipolar in each hemisphere in the model. On the Sun, the weak fields outside the polar regions are mixed polarity, thus limiting the extent of the open field area in possible coronal hole extension footprints. The amount of open field area also depends on the concentration of the polar fields, with less for more highly peaked polar distributions. Thus the modeled coronal hole footprints should be regarded only as an approximate envelope within which actual coronal hole footprints could appear.

The results in Figure 2, for an equatorial bipole, suggest that depending on the active-region bipole axis tilt, the helmet streamer belt may be pinched, warped out of the equatorial plane, or expanded into a broad triple arcade structure. To understand these differences, one can make comparisons with Earth's magnetosphere where the field configuration and solar wind interaction depend critically on the north–south component of the interplanetary magnetic field (Dungey, 1961). In the present coronal field model, the background solar field replaces the interplanetary

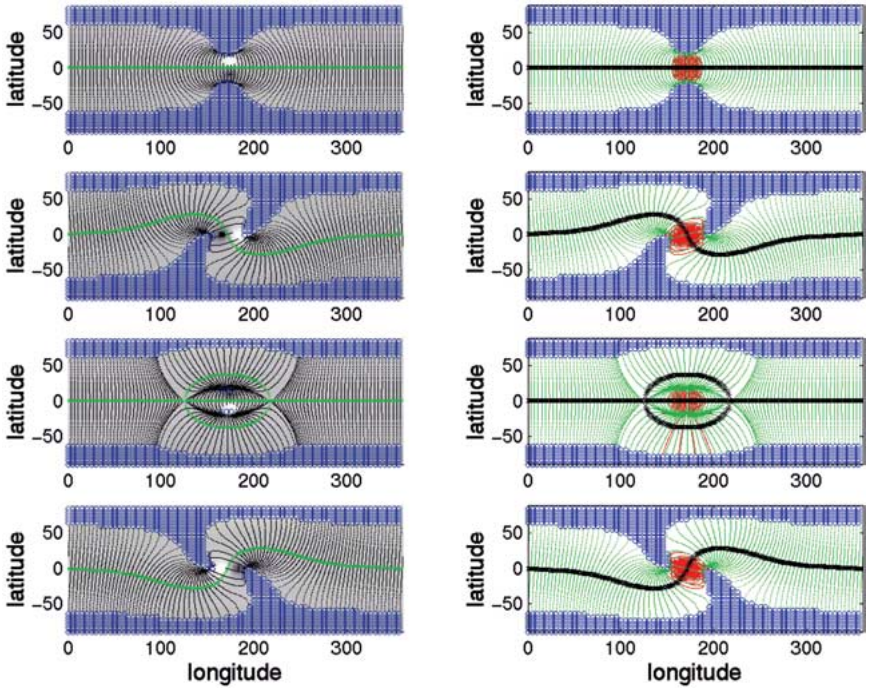

Figure 2. Synoptic display of the potential-field source-surface model results for a case with a single bipolar active region at the equator. The *panels on the left* show the constructed photospheric field in gray scale, with *black* and *white* indicating opposite inward and outward radial fields as in a standard magnetogram, with the modeled field lines of the helmet streamer belt (*black*), the source surface neutral line (*green*), and the footpoints of the open fields (*blue*) superposed. The *top panel* is for a bipole whose moment is parallel to the background polar field (southward or −90 deg tilt), the *third panel* is for a bipole antiparallel to the background field (northward or 90 tilt), and the remaining two panels show the results for east–west (180 deg tilt) and west–east (0 deg tilt) bipole axis orientations. The *righthand panels* show the corresponding displays with the active-region field lines highlighted in *red* to show their connectivities. In these plots the helmet streamer field lines are shown in *green* and the source surface neutral line in *black*.

field, and the active region bipole replaces the Earth's dipolar field. When the active region bipole has its moment parallel to the direction of the background field (top panel, Figure 2), a relatively benign interaction takes place that acts to further confine the active region fields within the helmet streamer belt arcade. When the bipole moment is antiparallel to the background field (third panel, Figure 2), the helmet streamer belt locally undergoes a major reconfiguration. In fact the trifurcated streamer belt is similar to the field configuration that plays the critical role in the CME concept of Antiochos, DeVore, and Klimchuk (1999). This trifurcation does not occur if a background field with a less-concentrated dipolar latitude dependence is assumed.

Figure 3 shows the modifications that occur when the bipolar region is instead placed at 30 deg north latitude. In this case the antiparallel bipole moment (third

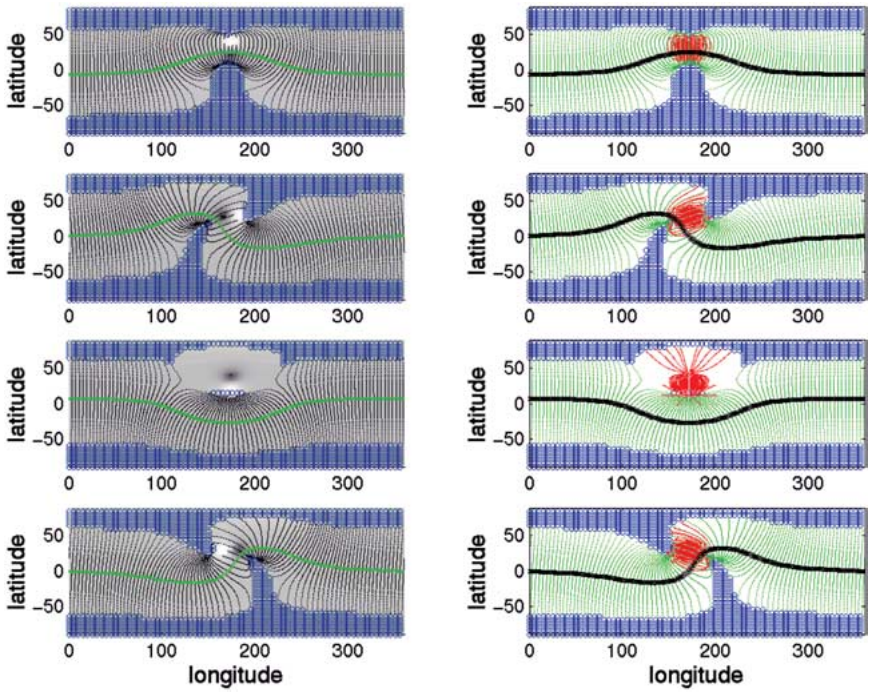

Figure 3. Same as Figure 2 but for a bipolar active region located at 30 deg N latitude. Areas such as that in the third panel from the top, which lie outside of both the open field region and the helmet streamer belt arcade, signify the existence of a separate helmet structure. In this case the separate helmet structure contains the active region in a manner resembling Figure 1(a).

panel) produces a detached closed field region, analogous to the separate coronal field helmets mentioned earlier. These helmets exist in unipolar open field regions, and in this case the helmet peak or cusp lies within the source surface. If the active region is stronger, or the polar field is more concentrated, this separate helmet can reach the source surface where it produces a ring-shaped isolated neutral line adjacent to the helmet streamer belt neutral line (e.g., as in a transition from the configuration in Figure 1(a) to that in Figure 1(b)). One can view the production of these separate helmets as an instability threshold of sorts, since a new magnetic cell is suddenly created in the corona as the active region bipole moment becomes sufficiently antiparallel. The separate helmet is moreover unburdened from the over-arching helmet streamer fields, suggesting a type of 'breakout'. As in the equatorial bipole case, significant differences in the coronal field configuration result from the presence of antiparallel fields and their associated nulls and separatrices. While the outcome of these modeled interactions are constrained by the current-free assumption and spherical source surface, the general idea of the differences between the parallel and antiparallel interactions is likely to be present in more sophisticated models. The simplified results are worth comparing with

observed CMEs to see if they are consistent with the appearance of their coronal contexts.

4. Comparisons with Observations

Figure 4(a) shows the SOHO MDI magnetograms for Carrington rotations (CRs) 1912–1917, during which a single large old-cycle active region at about −15 deg latitude dominated the photospheric field outside of the polar regions. Note that the major active region in CR 1917 is actually a different one than in the earlier Carrington rotations, but its general location and effects are similar. Examination of the active region in high-time-cadence (96 min) MDI full-disk data as it crossed the solar disk suggests it is evolving through diffusion, convection, and flux cancellation. In Figure 4(b), potential-field source-surface models for these Carrington rotations, derived from Mt. Wilson Observatory synoptic maps (C. N. Arge, personal communication) illustrate the related coronal hole footprints, helmet streamer belts, and source-surface neutral lines. All of these show evolving double coronal hole extensions and a warped helmet streamer belt like that in the second panels of Figures 2 and 3.

The predominant change in the scalar field observations in Figure 4(a) from Carrington rotation to Carrington rotation appears as an evolution of an initially east–west bipole to a pair of inclined, elongated unipolar regions (also see Mackay, Priest, and Lockwood, 2002). As suggested in Figure 5, this change can be viewed as an effective tilting of the old cycle region bipole moment in a direction that produces an increasingly antiparallel configuration with respect to the background field. This sheared bipolar region persisted for at least three solar rotations, after which it was supplanted in importance by a new bipolar active region closer to the equator and a few tens of degrees east. By CR 1917, three old cycle bipoles shared the photosphere, implying that the coronal field became subject to a more complicated control system.

The illustration in Figure 5 assumes bipolar region evolution starting from east-west alignment, which mimics the period of our example. However, when active regions emerge, their tilts typically follow Joy's law (Zirin, 1998), which implies their moments initially have a component antiparallel to the large-scale polar field. Variations of the tilts of newly emerging bipolar regions may in fact affect the corona's response to them, but analysis of that question is beyond the scope of this study. However, a potentially important consideration is that new cycle bipoles with emerged antiparallel components evolve with differential rotation so as to reduce their antiparallelness. This is in contrast to the present case, and may be an important factor in determining which bipolar regions give rise to recurring eruptions.

Figure 6, patterned after Figures 2 and 3, illustrates how the coronal field changes for an old-cycle bipole at −15 deg latitude that is oriented antiparallel (e.g., at

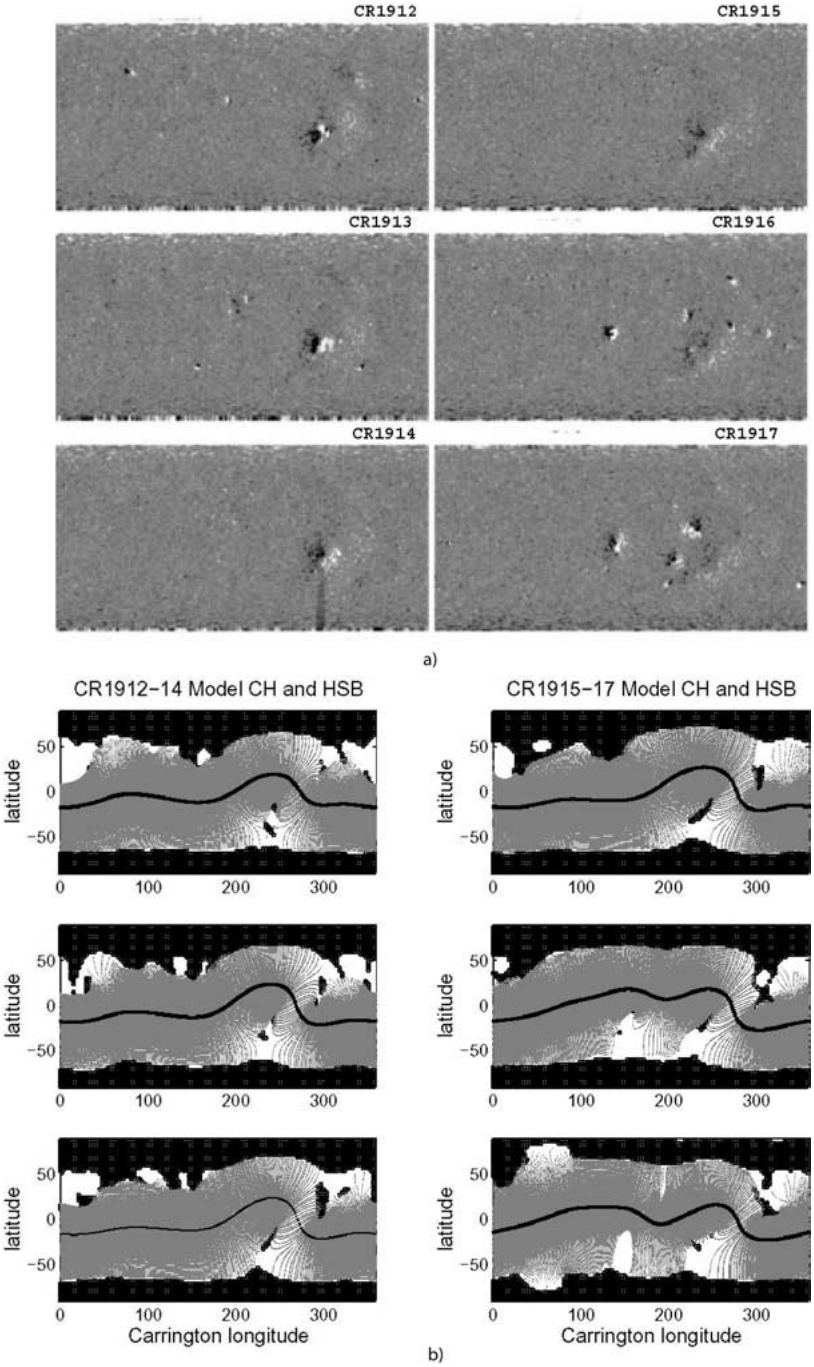

Figure 4. (a) SOHO MDI synoptic maps for Carrington rotations (CR) 1912 through 1917, showing the single large active region that dominated the photosphere until CR1917. (b) Potential-field source-surface model helmet streamer belt (HSB) field lines (*gray*), coronal hole (CH) footprints (*black*), and source surface neutral lines for the Carrington rotations shown in (a).

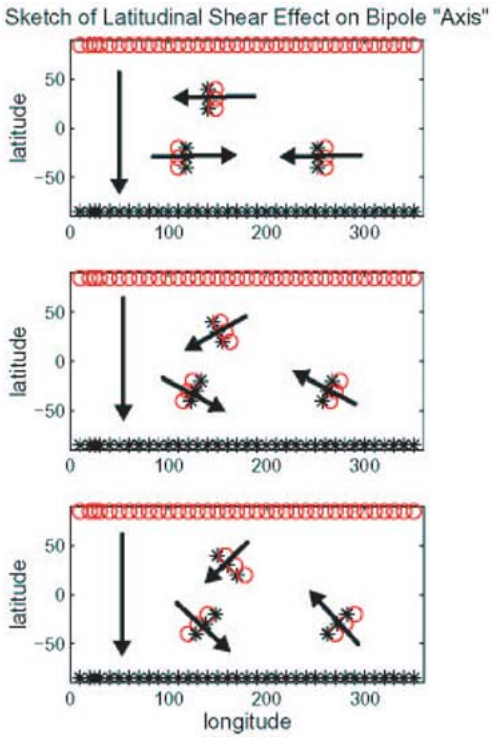

Figure 5. Illustration of how a decaying bipolar active region on the photosphere, like that in Figure 4, undergoes an effective change in axis orientation with time due to diffusion and differential rotation. For an old-cycle bipole such as that in the lower left, this evolution can result in the ongoing production of antiparallel components between the bipole's field and the polar photospheric background field. Of course, in general apparent antiparallel components can also be produced by flux emergence and other types of flux redistributions.

90 deg tilt) to the background polar field, and then at 60, 30, and 0 deg tilt angles with respect to east from top to bottom. As in the case shown in Figure 3 for the 30-deg latitude bipole and the antiparallel condition, the active region 'breaks out' of the helmet streamer belt to form a separate helmet for the 60-deg and antiparallel (90-deg tilt) orientations. The helmet streamer belt is also warped in a characteristic way around the separate helmet. These configurations can be compared with SOHO coronagraph observations to determine if the particular coronal field configuration associated with the breakout of the active-region helmet looks anything like the images during CMEs.

The right panels in Figures 7–9 show a few examples of CMEs observed by the SOHO LASCO-C2 coronagraph during the Carrington rotations dominated by the single bipolar active region. The CMEs on 22 August, 26 September, and 5 November 1996 were selected in part because of their clear loop-like signatures in the images, and in part because they show three different perspectives. On the left are spherical projections of the potential field model with the bipolar active region

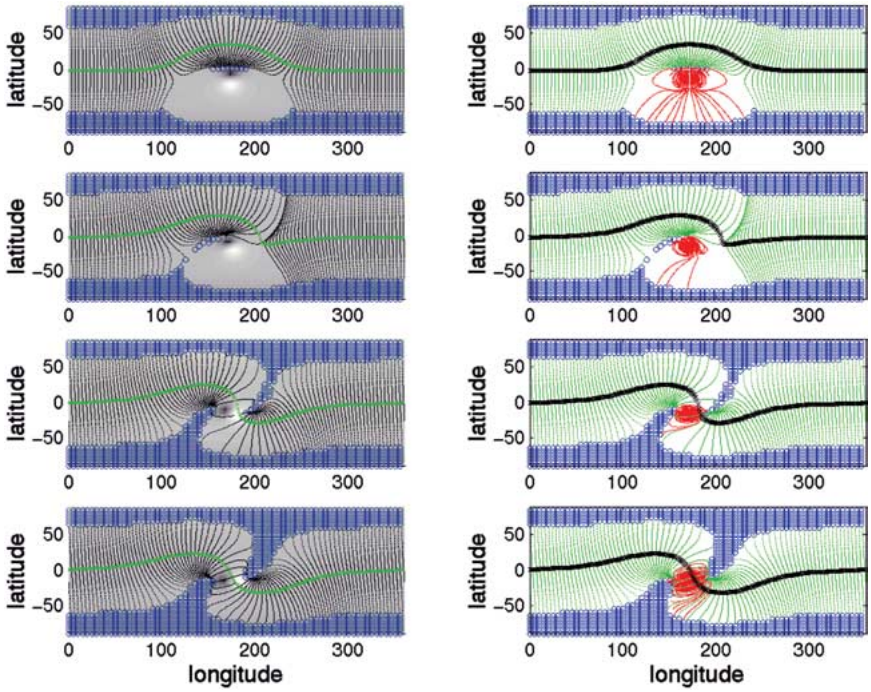

Figure 6. Same as Figure 2 but for an old-cycle bipole like that in Figure 4 at about −15 deg latitude. The bipole axis in this case has been rotated through four equally spaced angles between antiparallel (*top panel*) and eastward (*bottom panel*). Notice that the separate helmet structure (see text description of Figure 3) has already formed at the orientation ∼30 deg from antiparallel.

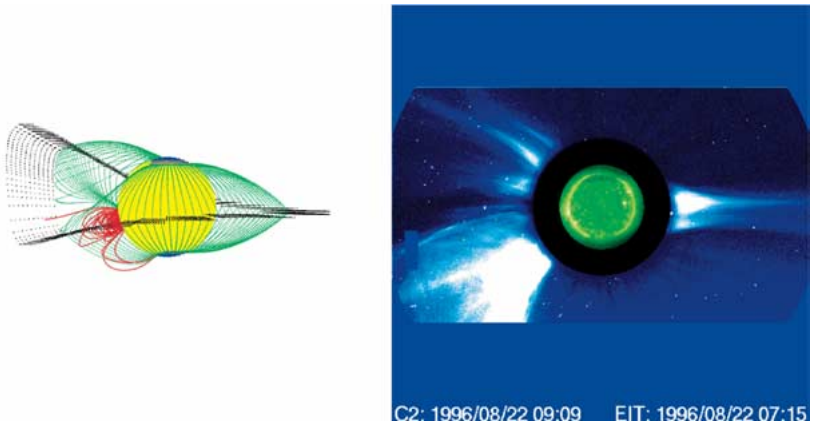

Figure 7. Comparison of a spherical projection of the model shown in Figure 6 with the image of a CME on 22 August 1996. The *black-dotted surface* is the radial extension of the source-surface neutral line, representing the base of the heliospheric current sheet and the plane around which the extensions of helmet streamer rays form.

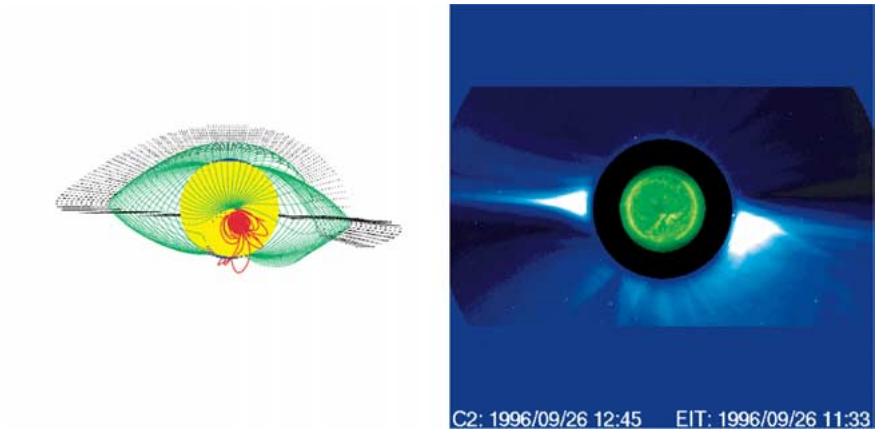

Figure 8. Same as Figure 7 but for 26 September 1996. This event was classified as a halo event in the CDAW CME list mentioned in the text.

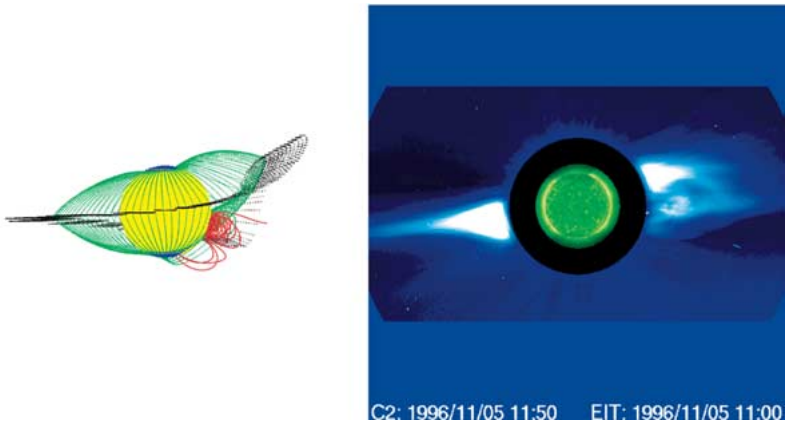

Figure 9. Same as Figure 7 but for the 5 November 1996 CME. In this case we use the same model even though the bipolar active region for this CME is the one in the map center for CR 1916 (Figure 4), which is slightly equatorward of its earlier counterpart.

at −15 deg south latitude oriented 60 deg from east to produce the antiparallel interaction. The global model has been rotated in each case to place the active region at approximately the correct longitude with respect to the viewer. Red field lines are again traced from the strong fields of the active region as in Figures 2 and 3. The beginnings of the heliospheric neutral sheet emanating from the source surface neutral line is shown as a black-dotted surface. This surface should coincide with the outermost coronal streamer structures seen in the LASCO-C2 images. Although the dynamics of the CMEs cannot be simulated with this model, the coronal context of the eruption, including deflected helmet streamers and the relative location of the fields associated with the active region and the helmet streamer belt, are suggested by the model topology.

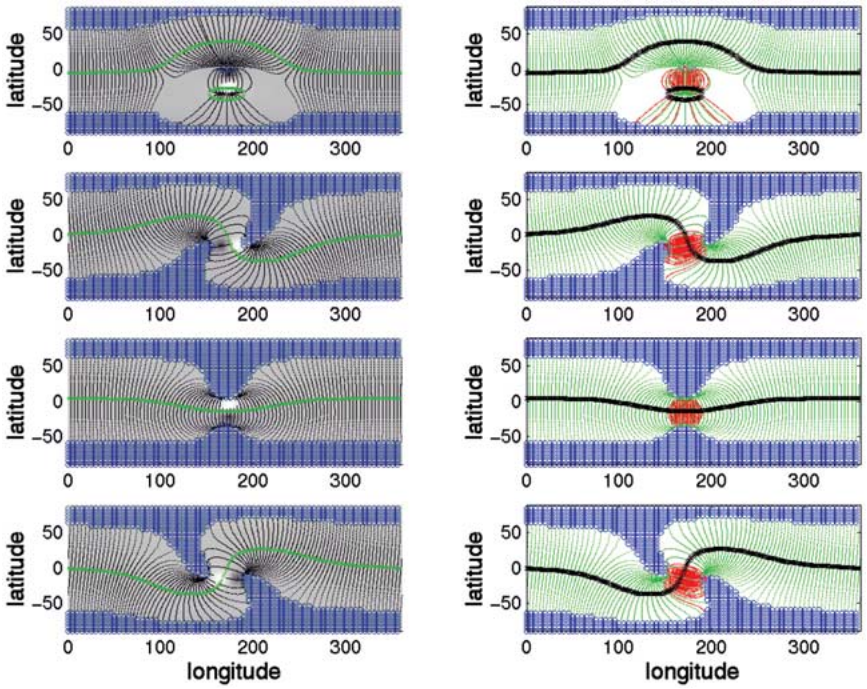

Figure 10. Same as Figure 6 but for an active region that is 40% stronger. In this case a ring-shaped source-surface neutral line forms at the apex of the separated helmet streamer as in Figure 1(b) when the bipolar active region axis is antiparallel (*top panel*).

The ring-shaped source surface neutral line feature mentioned earlier is not present in the model version compared with the CMEs above, but it appears if the active region is made $\sim 40\%$ stronger, as seen in Figure 10 (top panel). This feature, shown in spherical projections in Figure 11(a), produces a secondary current sheet/streamer formation that resembles a partial halo in coronagraph images. A similar impression results for the spherical projections of the antiparallel equatorial bipole case in the third panel of Figure 2. Figure 11(b) illustrates the centered and symmetrical halo-like appearance of the secondary current sheet/streamer in that model. A characteristic of both of these configurations is that the 'halos' exist in addition to the regular helmet streamer belt/current sheet structure – in accord with the appearance of some halo observations.

5. Cases with More Bipolar Active Regions

When other bipoles are added to the photosphere, the variety of possible behaviors, of course, increases exponentially. One double active region case of special interest involves active regions across the equator from one another. This configuration approximates a condition that occurs on the photosphere during the rising phase

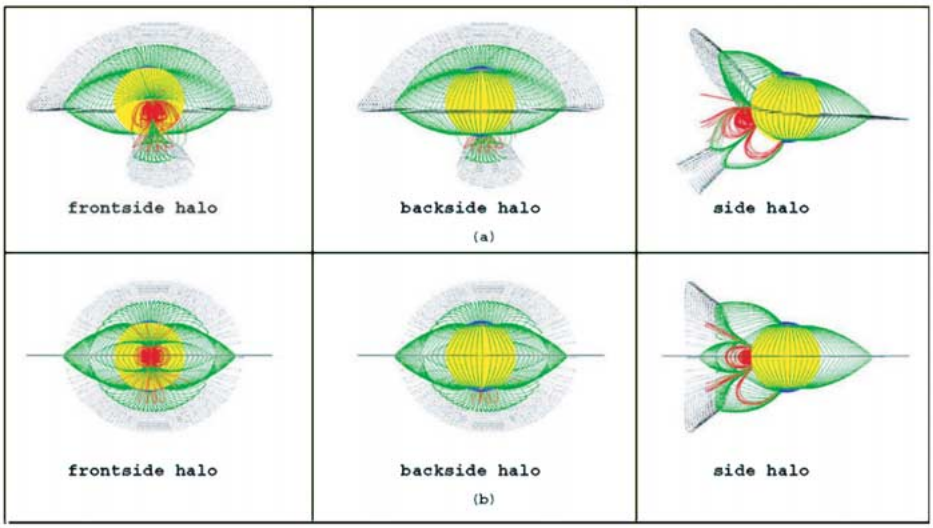

Figure 11. (a) Three spherical projections of the case shown in the top panel of Figure 10. The extension of the ring-shaped neutral line suggests a halo-like streamer structure could form under conditions when the bipole is antiparallel. (b) Similar displays as (a) but for the antiparallel equatorial bipole case in the third panel of Figure 2.

of the solar cycle when new cycle mid-latitude bipoles mingle with others in the opposite hemisphere of either new or old cycle polarity.

The results of a model calculation analogous to that in the preceding section, with bipoles at 30 deg north and south latitudes, in this case with only the northern hemisphere bipole rotating through the four axis tilts, are illustrated in Figures 12 and 13. Some particularly interesting features are produced when the bipoles are horizontal but antiparallel to one another, as in the top panel of Figure 12. The helmet streamer belt in this case takes on the split streamer configuration of Figure 2, the case of the equatorial antiparallel bipole, except that its centroid is displaced from the active region longitudes. To the right of this split section is a pinched section of streamer belt. Evidently, the corona perceives this active region pair as two bipoles with north–south axes, one antiparallel and one parallel to the background field. The result is a hybrid of the two analogous single bipole cases for parallel and antiparallel axes in the top and third panels of Figure 2. As suggested by the spherical projections in Figure 13, this double active region model also produces cross-equatorial field arcades connecting the active regions, as seen in some CME event coronal observations (e.g., Delannée and Aulanier, 1999), and a halo-like feature like those described above. A notable property of this configuration is that it involves current cycle (Hale's law) orientations of low inclination bipoles.

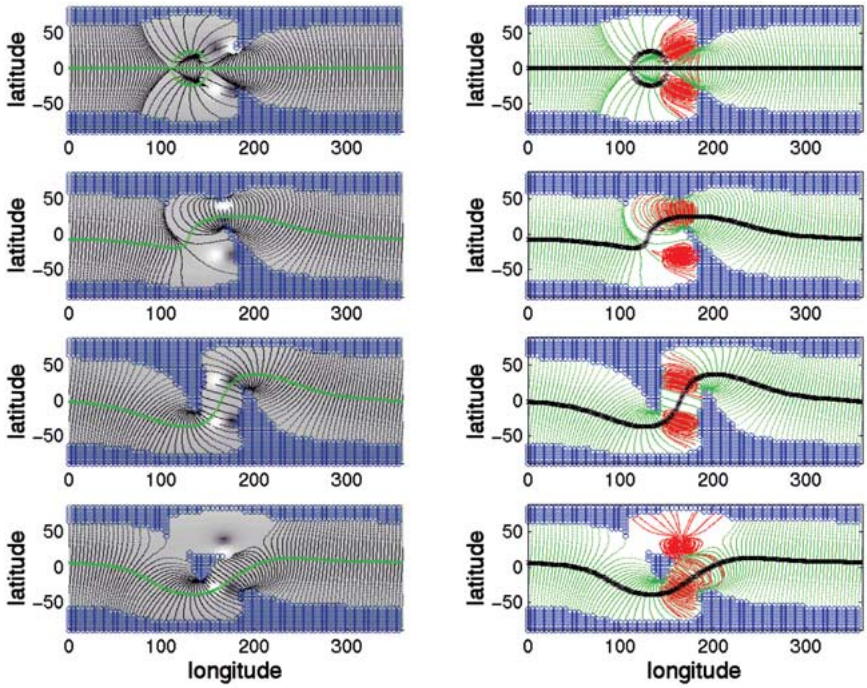

Figure 12. Same as Figure 2 but for two bipolar active regions placed at 30 deg north and south of the equator, at the same longitude. The northern bipole is rotated through 270 deg to sample the range of coronal field structure that could result. In the *top panel*, the oppositely directed (Hale leading polarity) bipoles seem to pair up in the model to produce a hybrid between the single parallel and antiparallel bipole cases shown in the top and third panels of Figure 2. Cross-equator arcades connect the active regions in the *top* and *bottom panels*.

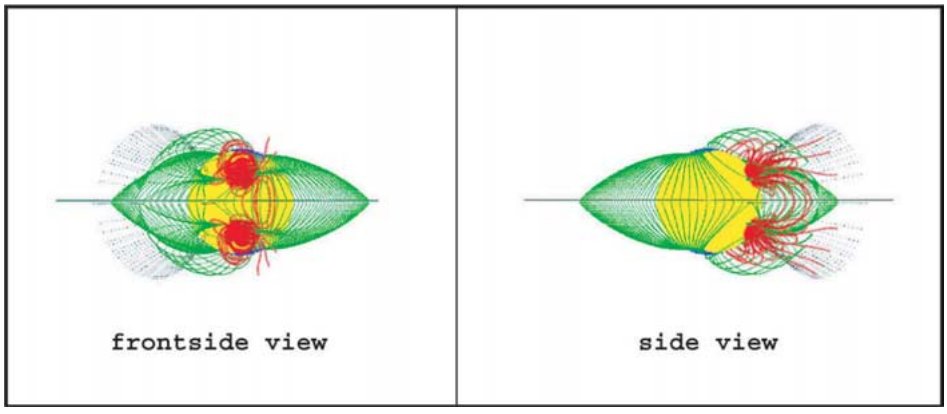

Figure 13. Two spherical projections of the case shown in the top panel of Figure 12.

6. Discussion

What is most constraining in these comparisons is the model's simplistic representation of the active region and the assumption of a steady state, current-free interaction with the background corona. We have used standard synoptic maps from observations to verify the general coronal field geometry produced by the potential-field model, but they do not capture the extent of the bipolar axis tilting effects that we have experimented with here. Thus if the general idea of antiparallel fields in active region interactions with the larger-scale coronal fields is accurate, the effect in magnetograms is either short-lived or involves antiparallel components from nonpotential active region fields that are invisible in scalar photospheric magnetograms.

On the positive side, we know from many previous studies that the potential-field source-surface model provides remarkably good descriptions of the inferred coronal field structure, and that the reconfigurations suggested here are not unreasonable for the observed distributions and evolution of active regions. Such reconfigurations could affect the magnetic support system for prominences in the neighborhood as suggested by Wang and Sheeley (1999), leading to CME-related prominence eruption or collapse. The trifurcated helmet streamer configurations found here are essentially those envisioned by Antiochos, DeVore, and Klimchuk (1999) in the breakout model of CMEs. Moreover, they lead to additional source surface neutral lines and their associated current sheets and streamers that might explain the appearance of coronagraph image halos. The prospect of repeated eruptions spawned by a bipolar region that maintains or regenerates its antiparallel components is also attractive considering the sequence of CMEs occurring during CR 1912–1917.

The above analysis is based on simple, yet realistic photospheric fields for near solar-minimum conditions. Throughout much of the solar cycle the fields are more complicated, with both ephemeral and longer-lived active regions emerging and fading on different time scales against a background of mixed-polarity quiet-Sun field and generally unipolar polar cap fields. The bipolar active regions at mid-latitudes usually have the current cycle polarity in their leading patch (with respect to solar rotation), while the low-latitude regions often show the old-cycle polarity leading. However, there is sometimes a mixture, and proximate active regions sometimes form marriages that result in confused partnerships and leading polarities. Occasional delta-spot active regions and other more complex systems involving sunspots certainly introduce active-region-scale structures full of null points and antiparallel fields even without the interaction with their surroundings considered. Nevertheless, the basic ideas described here could still apply on the larger scale. Effective bipoles produced by pairings of proximate large-scale photospheric field concentrations from separate emergence episodes can produce the same effects in the corona as congenital bipolar regions.

Further investigation of these ideas requires a global coronal MHD model that uses similar boundary conditions and assumptions to investigate coronal field structure and its sensitivities. The key requirements identified here that have not yet been applied to such MHD models are: (1) a background field that is concentrated at the poles much more than a dipole field, (2) bipolar active regions whose axial tilts are varied from parallel to antiparallel to the local background field, ideally as a time-dependent boundary condition, and (3) combinations of active regions that are sufficiently proximate to interact with each other, especially across the equator, during some of the numerical 'experiments'. Indeed, the problem needs MHD coronal models that while not perfect in their other details, allow the next improvement over potential field source surface modeling of the basic time-dependent coronal field structure for arbitrary photospheric fields. These need to be simple and streamlined enough to allow one to experiment with hypothetical photospheric field patterns and their resulting coronal changes. It is hard to imagine making substantial progress without such a tool.

Acknowledgements

The above work was partially supported by grants 164766 from the National Science Foundation Space Weather Program and by the Solar MURI Project at UC Berkeley sponsored by the Air Force Office of Scientific Research. We thank the SOHO LASCO and EIT investigation teams for making their images available through their websites. The SOHO mission is a joint ESA/NASA cooperation. We similarly thank the Mt. Wilson Observatory group, and Nick Arge at NOAA-SEC and CERES, University of Colorado, for making photospheric field synoptic map data available.

References

Altschuler, M. D., Levine, R. M., Stix, M., and Harvey, J.: 1977, *Solar Phys.* **51**, 345.
Antiochos, S. K.: 1998, *Astrophys. J.* **502**, L181.
Antiochos, S. K., DeVore, C. R., and Klimchuk, J. A.: 1999, *Astrophys. J.* **510**, 485.
Aulanier, G. *et al.*: 1999, *Astron. Astrophys.* **342**, 867.
Beveridge, C., Priest, E. R., and Brown, D. S.: 2002, *Solar Phys.* **209**, 333.
Bungey, T. N.: 1995, Ph.D. Thesis, St. Andrews University.
Delannée, C. and Aulanier, G.: 1999, *Solar Phys.* **190**, 107.
de Toma, G., White, O. R., and Harvey, K. L.: 2000, *Astrophys. J.* **529**, 1101.
Dungey, J. W.: 1961, *Phys. Rev. Lett.* **6**, 47.
Falconer, D. A.: 2001, *J. Geophys. Res.* **106**, 185.
Feynman, J. and Martin, S. F.: 1995, *J. Geophys. Res.* **100**, 3355.
Forbes, T.: 2000, *J. Geophys. Res.* **105**, 153.
Gibson, S. E. *et al.*: 1999, *Astrophys. J.* **520**, 871.
Harrison, R. A., Hildner, E., Hundhausen, A. J., Sime, D. G., and Simnett, G. M.: 1990, *J. Geophys. Res.* **95**, 917.

Lewis, D. J. and Simnett, G. M.: 2000, *Solar Phys.* **191**, 185.
Li, Y., Luhmann, J. G., Mulligan, T., Hoeksema, J. T., Arge, C. N., Plunkett, S. P., and St. Cyr, O. C.: 2001, *J. Geophys. Res.* **106**, 103.
Linker, J. A. and Mikić, Z.: 1995, *Astrophys. J.* **438**, L45.
Longcope, D. W. and Kankelborg, C. C.: 2001, *Earth, Planets Space* **53**, 571.
Luhmann, J. G., Gosling, J. T., Hoeksema, J. T., and Zhao, X.-P.: 1998, *J. Geophys. Res.* **103**, 6585.
Mackay, D. H., Priest, E. R., and Lockwood, M.: 2002, *Solar Phys.* **207**, 291.
Mikić, Z., Linker, J. A., Schnack, D. D., Lionello, R., and Tarditi, A.: 1999, *Phys. Plasmas* **6**, 2217.
Priest, E. R.: 2001, *Earth, Planets Space* **53**, 483.
Priest, E. R. and Schrijver, C. J.: 1999, *Solar Phys.* **190**, 1.
Sheeley, N. R., Wang, Y-M., and Harvey, J. W.: 1989, *Solar Phys.* **119**, 323.
Sime, D. G.: 1989, *J. Geophys. Res.* **94**, 151.
Subramanian, P. and Dere, K. P.: 2001, *Astrophys. J.* **561**, 372.
Usmanov, A. V.: 1995, *Space Sci. Rev.* **72**, 121.
Wang, Y.-M. and Sheeley, N. R., Jr.: 1992, *Astrophys. J.* **392**, 310.
Wang, Y.-M. and Sheeley, N. R., Jr.: 1993, *Astrophys. J.* **414**, 916.
Wang, Y.-M. and Sheeley, N. R., Jr.: 1999, *Astrophys. J.* **510**, L157.
Wang, Y.-M. and Sheeley, N. R., Jr.: 2002, *J. Geophys. Res.* **107**, 2001JA000500.
Wang, Y.-M. *et al.*: 1997, *Astrophys. J.* **485**, 875.
Webb, D. F. *et al.*: 1997, *J. Geophys. Res.* **102**, 161.
Wu, S. T., Andrews, M. D., and Plunkett, S. P.: 2001, *Space Sci. Rev.* **95**, 191.
Zhao, X.-P. and Webb, D.F.: 2002, *J. Geophys. Res.*, in press.
Zirin, H: 1998, *Astrophysics of the Sun*, Cambridge University Press, Cambridge.